Fábricas magnéticas y análisis cuantitativo de texturas mediante difracción neutrónica de tiempo de vuelo: ejemplos en tectonitas (NO del Macizo Ibérico, España).

Magnetic fabric and quantitative texture analysis using Time-of-flight neutron diffraction: Examples in tectonites (NW Iberian Massif, Spain)

Juan GÓMEZ BARRERIRO[(1)], Fernando ÁLVAREZ LOBATO[(2)]

[(1)] Dpto. de Petrología y Geoquímica – Instituto de Geología Económica CSIC
Universidad Complutense de Madrid
jgomezbarreiro@gmail.com

[(2)] Dpto. de Geología
Universidad de Salamanca
fernando@usal.es

Received: 31/03/2010
Accepted: 30/06/2010

RESUMEN
La orientación cristalográfica preferente o textura es una característica intrínseca a los materiales cristalinos como las rocas y tiene una influencia determinante en las propiedades físicas de las mismas, principalmente en la anisotropía. Su caracterización debe realizarse con métodos cuantitativos, preferiblemente aquellos que recojan una información volumétrica del agregado. La difracción neutrónica permite analizar grandes volúmenes de muestra debido a la baja absorción de los neutrones por la materia cristalina. La información sobre la distribución de orientaciones así obtenida puede emplearse para calcular las propiedades físicas del agregado, como la susceptibilidad magnética, ponderando las propiedades del monocristal por todo el espacio de orientaciones. En el caso particular de la anisotropía de la susceptibilidad magnética (ASM) el éxito de tales cálculos está determinado por la disponibilidad de caracterizaciones precisas del tensor ASM de cada fase mineral y su relación con la red cristalina. Para la mayor parte de los principales minerales estas relaciones se ven complicadas por la baja simetría de las redes cristalinas (monoclínicas-triclínicas). Parte de la ambigüedad derivada de esta cuestión puede resolverse combinando el análisis de texturas, la simulación de ASM y la realización de experimentos de ASM. En el presente estudio mostramos varios ejemplos en los que aplicamos esta metodología a la resolución de problemas microestructurales encontrados en tectonitas del NO del Macizo Ibérico.
Palabras clave: Análisis de texturas, difracción neutrónica, ASM, zonas de cizalla, Macizo Ibérico.

ABSTRACT
Crystallographic preferred orientation or texture is an intrinsic feature of crystalline matter. Texture determines physical properties of rocks, particularly anisotropy. Texture analysis should rely on quantitative methods, which provide 3D information of the aggregate. Neutron diffraction has notorious advantages because of high penetration in geomaterials, so large sample volume can be analyzed. Orientation distribution of crystals in the aggregate can be used to calculate physical properties of the rocks, like magnetic susceptibility, by averaging single crystal properties over the orientation distribution. Calculations of the anisotropy of magnetic susceptibility (AMS) have to be based on accurate correlation of the AMS single crystal data and crystal lattice. However, most of rock-forming minerals have low symmetry lattices (monoclinic-triclinic), consequently that correlation is complex. We can partially overcome those difficulties combining texture analysis, AMS simulation, and direct measurement of AMS. We present four examples of tectonites from NW Iberian Massif, where microstructural issues have been solved following that methodology.
Key words: Quantitative texture analysis, neutron diffraction, AMS, shear zones, Iberian Massif

1. INTRODUCTION

Many natural and synthetic materials are crystal aggregates with a non-random distribution of orientations. It is said that these aggregates show preferred orientation or 'texture'. In such materials many physical properties are anisotropic, they depend on direction (e.g., Kocks et al. 2000). In order to predict material properties one must analyze both the anisotropy of most single-crystal properties and the non-randomness nature of crystal orientation distribution in the aggregate (e.g. Wenk, 1985; Kern, 1993;Wenk and Van Houtte, 2004). Rocks are aggregates of minerals, i.e. polycrystals, and the arrangement of those crystals determines their microstructure. In Earth sciences understanding of (micro)structure/property relations is a cornerstone to interpret rock features in kinematic and dynamic terms. Moreover,, macroscopic properties may result in distinct geophysical response of rocks, so unequivocal correlation has to be done between texture and anisotropy for deep Earth exploration (e.g. Savage, 1999; Gómez Barreiro et al. 2007).

Anisotropy is recognized in most of the crustal rocks and parts of the mantle (e.g. Christensen, 1971; Kern and Wenk, 1985; Nicolas and Christesen, 1987; Wenk et al. 2008; Karato, 1998; Babuška and Plomerová, 2006; Park and Levin, 2002; Savage and Silver, 1993; Tarling and Hrouda, 1993; Savage, 1999; Mainprice et al. 2000). Anisotropy of thermal and elastic properties determines geodynamic processes in Earth. Consequently, we have to understand the parameters which control such behavior to properly model and interpret solid earth evolution. Several factors control anisotropy, like temperature, pressure, stress, strain, fluid activity and chemical composition. Their interactions lead to mineral changes and the development of different arrangements of rock components. Whatever the primary/secondary process that unbalances the rock state, changes in preferred orientation of minerals can modify the relation between stimulus and response of the rock.

We focus here on the correlation of anisotropy of magnetic susceptibility (AMS) and the crystallographic preferred orientation (CPO) or texture of tectonites. The mineral composition of tectonites which developed under metamorphic conditions in the crust is dominated by feldspars, quartz, amphiboles and sheet silicates. Feldspars and quartz show a diamagnetic behaviour while amphiboles and micas present a paramagnetic response (e.g. Borradaile et al., 1987; Uyeda et al. 2000; Martín-Hernández et al. 2004). The interpretation of AMS in structural terms of resulting rock types: metabasites, schists and quartzites, has to rely on previous identification of what mineral phases are contributing to the bulk AMS (e.g. Cifelli et al., 2009). In some cases, the presence of inclusions and/or accessory minerals with ferromagnetic (s.l.)behaviour (e.g., magnetite) may distort the magnetic fabric of major phases (e.g. Lagroix and Borradaile, 2000). Ultimately, all physical properties depend on crystal structure and atom-scale interactions. As a consequence, magnetic properties of single crystals have to be constrained before any interpretation of AMS in terms of microstructure (Borradaile and Jackson, 2004). Precise correlation of crystal lattice and AMS is difficult due to the low symmetry of most common phases (e.g. triclinic, monoclinic) whereas AMS is always orthorhombic.

The CPO or texture of tectonites is related to the deformation history of the rock. Symmetry of textures in combination with microstructural analysis of natural and experimentally deformed aggregates leads us to infer kinematic and dynamic information of structural events. Interestingly, detailed inspection of the orientation distribution of crystal directions and planes with respect to the tectonite reference system (foliation and lineation) allows us to discuss the activity of different mechanisms during deformation (e.g. slip systems; Wenk and Christie, 1991). Techniques for texture analysis include, on the one hand, single grain methods, like the Universal Stage (U-Stage) and Electron Back-Scattered Diffraction (EBSD), and on the other hand, volume methods, like neutron and X-ray diffraction (e.g. Siegesmund et al., 1994; Ullemeyer et al 2000, Xie et al., 2003). Both single grain and volume methods have advantages and limitations to be considered. Single-grain methods are well suited for microstructure/texture correlation, but grain statistics are limited, and low symmetry phases, like triclinic plagioclase, may not be totally solved (Prior et al., 1999; Gómez Barreiro et al., 2007). Volume methods, particularly high-energy X-rays (Synchrotron) and neutron diffraction, analyze larger volume samples, and lead us to resolve the texture of assemblages of low-symmetry minerals (Leiss et al. 2002; Wenk and Grigull, 2003; Lonardelli et al. 2005; Wenk et al., 2008; Gómez Barreiro et al., 2010). In all cases, the goal of those techniques is to obtain a quantitative orientation distribution (OD) of each mineral in the aggregate. The OD can be used to model physical properties of the rock through several averaging schemes (Owens, 1974; Wenk, 1985; Mainprice and Humbert, 1994; Siegesmund et al., 1995; Martín-Hernández et al. 2005; Schmidt et al. 2009), so that the contribution of each mineral to a specific property can be determined.

We present some preliminary results from tectonites of the NW Iberian Massif (NW Spain) (Fig.1). Distinct structural contexts illustrate the combination of AMS,

texture analysis and texture derived physical properties (AMS) to solve microstructural questions.

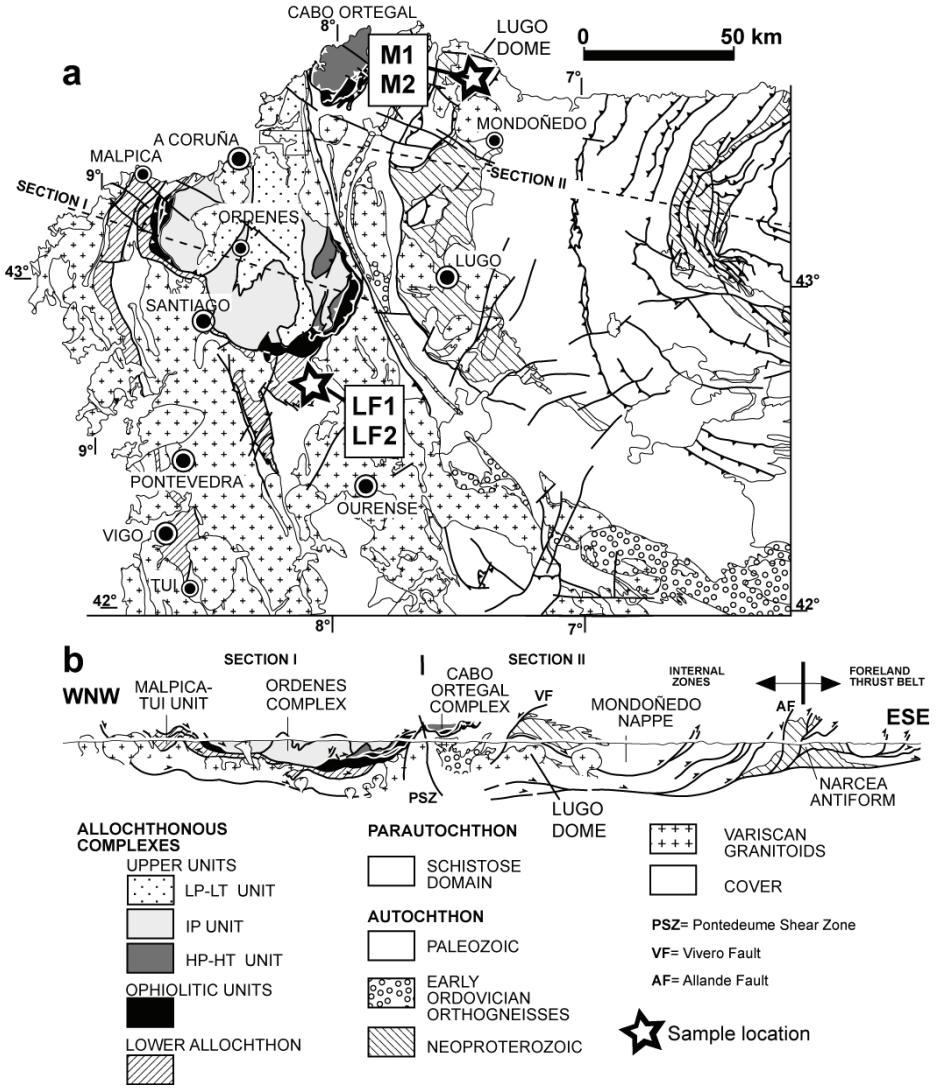

Figure 1. a) Geological map of the NW Iberia. Samples and geological cross sections are indicated. b) Geological cross sections of the NW Iberia. Principal tectonometamorphic units are labeled.

2. GEOLOGICAL CONTEXT, SAMPLE DESCRIPTION AND PREPARATION

2.1. Basal thrust of the Lower Allochthon (Órdenes Complex)

The Basal Allochthon is a thrust sheet structurally located at the bottom of the Órdenes Complex (Fig. 1). Tectonometamorphic evolution includes evidence of a subductive event during Variscan Orogeny (360 Ma), followed by exhumation through recumbent folds and ductile thrusts to the E (present coordinates) during collisional stages (345 Ma) and extensional collapse at 315 Ma (Martínez Catalán et al., 2009; Díaz Fernández and Martínez Catalán, 2009: Gómez Barreiro et al., 2010). Ductile thrusts and recumbent folds show complex relationships resulting in controversial interpretation of lineations (Hobbs et al., 1976). In this context, geometric relationships of lineations have to be statistically evaluated across the unit. We focused on mylonites from the basal thrust. Texture and AMS was evaluated in reference rock types (metabasites and quartzites) in order to correlate mineral and magnetic fabrics before extensive AMS measurement across the unit.

Description of pilot samples

LF1: Mylonitic quartzite from the basal thrust of the Lower Allochthon (Órdenes Complex, Fig.1; Martínez Catalán et al., 2009). Mineral composition includes quartz (78%) and muscovite (22%). Quartz appears dynamically recrystallized, with evidence of moderate grain boundary migration and subgrain rotation. Quartz appears moderately elongated defining a weak preferred shape orientation. Some grains show undulose extinction. Muscovite grains define the foliation with no evidence of internal deformation.

LF2: Mylonitic metabasite from the same location as *LF1*. It is a fine-grained amphibolite with a penetrative mylonitic fabric (L>S). A mixture of plagioclase (albite; 30%) and amphibole (hornblende; 65%) dominates the matrix with presence of minor (5%) epidote, titanite, quartz and garnet.

2.2. High-temperature shear zone (Lugo Dome)

Extensional collapse within basement sections of the autochthon of Variscan orogen was driven by ductile shear zones. In the Lugo Dome (Fig. 1), several shear zones were identified. Together with recent kinematic and structural analysis (e.g. Martínez Catalán et al. 2003) quantitative texture analyses were done in two distinct levels across the shearing gradient in the shear zone: active domains (*M1*), and passive domains (*M2*). Those domains reflect the strain partitioning during the evolution of the shear zone, with active volumes where deformation was preferentially accommodated. The geometrical relationship between fabric elements (lineation/foliation) of passive and active domains is important to decipher the behaviour of the shear zone (Hobbs et al. 1976). Recrystallization in both domains overshadows microstructural evolution. Extensive grain growth in passive domains deleted

mesoscopic foliation and lineation, and just very fine muscovite inclusions appeared to be aligned under the microscope. AMS analysis and CPO modeling was done to evaluate the correlation between magnetic and mineral fabrics in order to map the pre-recrystallization foliation in passive domains.

Description of pilot samples
M1: Mylonitic quartzite from a high temperature shear zone (Lugo Dome, Fig.1; Martínez Catalán et al. 2003). Mineral composition includes quartz (96%) and muscovite (4%). Quartz is dynamically recrystallized, with irregular boundaries and anisotropic shape defining a rough foliation. Muscovite is very fine-grained and variably oriented. Micro shear-bands (C') develop at an acute angle (10-35º) to the foliation, synthetic with the general top-to-the SE kinematic of the shear zone. Cylindric sample was drilled in a sector where shear band does not apparently form.

M2: Annealed mylonitic quartzite (same location that *M1*). In the high-temperature shearing context of *M1*, some boudins appear annealed. Mineral composition includes quartz (96%), orthoclase (2%), and muscovite (2%). Microstructure is characterized by an abnormal quartz grain growth (1 cm maximum), defining globular grains which include a previous fine grained foliation, now defined by very fine muscovite grains (5-50 μm). Feldspar occupies interstitial positions in the matrix. Previous CPO analyses suggested static growth with similar quartz texture patterns but weaker. Foliation is not visible in the field, but became apparent under the microscope.

2.3. Sample preparation
Cylindrical core specimens (height: 1 cm, diameter: 1 cm) were drilled perpendicularly to the foliation from oriented samples (Fig. 2), and used for both texture and AMS analyses. The sample reference system was kept on each specimen (or cylinder) (X//Lineation; XY// foliation; Z//foliation pole), with the cylinder axis being parallel to the foliation pole (Z), and cylinders top and bottom cut with a precision saw parallel to the foliation. An arrow parallel to the lineation trend was marked on top of each sample.

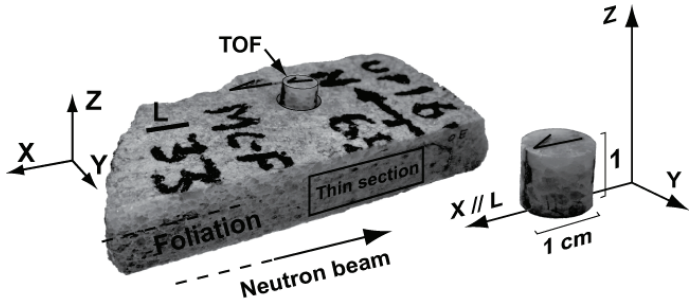

Figure 2. Sample reference system. Sample cylinder is drilled with the axis normal to the foliation. Arrow on top points to the mineral lineation. TOF: Time-Of-Flight

3. METHODOLOGY

3.1 Texture analysis

Experiments were done in the neutron Time-Of-Flight (TOF) diffractometer HIPPO (High-Pressure-Preferred-Orientation) at LANSCE and instrument optimized for texture analysis (Los Alamos Neutron Science Center; e.g., Wenk et al. 2003; Matthies et al., 2005; Vogel and Priesmeyer, 2006; Gómez Barreiro et al. 2007). Each oriented cylinder was fully immersed in the neutron beam. For each measurement, the sample was rotated around the cylinder axis (perpendicular to the incident neutron beam; Fig. 2) into three positions (0°, 45°, 90°) to improve pole figures angular coverage. .At each position, data were collected for 30 minutes resulting in a total exposure time of 90 minutes. TOF diffraction spectra (Figs. 4a to 7a) were analyzed with the Rietveld method as implemented in the software MAUD (Material Analysis Using Diffraction; Lutterotti et al. 1999). The orientation distribution (OD) resolution was 15º. The OD was exported from MAUD and then used in BEARTEX to calculate and plot pole figures (Wenk et al. 1998).

In the Rietveld refinement, crystallographic structures (CIF files) were required. For monoclinic phases two coordinate lattice systems can be used: with the 2-fold rotation axis, which is common to all point groups in the monoclinic system, defined parallel to **c** or **b** lattice vectors, resulting in first and second setting respectively. The first setting has to be used, both in MAUD and Beartex (Matthies and Wenk, 2009), which requires some transformations. For representations here we use labels for second setting (i.e. [010] is the 2-fold axis). It should be noted that due to the low crystal symmetry of some major components, e.g. hornblende, muscovite (monoclinic) and plagioclase (triclinic), [100] [010] and [001] directions do not correspond to the pole of the respective crystallographic plane (100) (010) (001), except for [010] in the monoclinic system. Poles of (20-1) (010) (-102) and (-401) (010) (-104) were used as the best approximation to [100] [010] and [001] directions for plagioclase and amphibole respectively (Xie et al. 2003; Gómez Barreiro

et al. 2010). In this work only those mineral phases relevant in terms of deformative fabric and magnetic anisotropy will be considered in detail. It should be noticed that important mineral phases in terms of magnetic fabric (e.g. magnetite) may be present in some samples, particularly in metabasites, well as submicroscopic grains in the matrix or included in other minerals. While these phases may raise the mean magnetic susceptibility of the rock, it is expected that, if present, the high magnetic anisotropy of major paramagnetic phases (i.e. amphiboles, micas) dominate the bulk anisotropy of the specimen (e.g. Borradaile et al., 1987).

3.2. AMS

Low-field AMS analyses were done at room temperature with a KLY-2 susceptibility meter (manufactured by AGICO, Brno) operating at an alternating weak field (4×10^{-4} T, 920 Hz and a resolution better than 5×10^{-8} SI) at the University of Salamanca. The magnetic susceptibility (k) is a symmetric second rank tensor that can be represented by an ellipsoid where the three principal axes are k eigenvalues ($k_1 \geq k_2 \geq k_3$ or $k_{max} \geq k_{int} \geq k_{min}$) (Fig. 3a.; Borradaile, 1988). Mean susceptibility is given by $k_M = (k_1+k_2+k_3)/3$. Anisotropy degree is represented by $P = k_1 / k_3$ (Nagata, 1961). Shape parameter is given by $T = (2 \ln k_2 - \ln k_1 - \ln k_3) / (\ln k_1 - \ln k_3)$ (Jelinek, 1981).

3.3. Calculation of theoretical AMS

Since the AMS of a rock results from the preferred orientation of magnetic minerals and their intrinsic magnetic anisotropy, the theoretical AMS of the textured aggregate can be calculated by averaging single-crystal magnetic anisotropy tensors over the entire volume of studied aggregate. Considering mineral composition and mean susceptibility (k_M) of the rocks, and single crystal magnetic properties, we have made the following assumptions: 1) magnetic susceptibility of *LF2* metabasite is dominated by a paramagnetic contribution which may be dominated by hornblende AMS ($k_{M\ \mathrm{Hbl}} = 8919 \pm 11 \times 10^{-6}$ SI; Borradaile et al., 1987), 2) *M1* and *M2* quartzites show a diamagnetic response. The AMS of quartz and orthoclase single crystals are considered to be near isotropic (Hrouda, 1986; Uyeda et al., 2000) so it is assumed that the observed anisotropy comes from muscovite grains (Fig. 3a). We used crystal densities of 3.28 g/cm^3 for hornblende and 2.82 g/cm^3 for muscovite.

Hornblende and muscovite single crystal AMS tensors from Borradaile et al. (1987) and Martín-Hernández and Hirt (2003) respectively, were used for calculations (Fig. 3). In monoclinic crystals some considerations have to be made: only one crystal axis is parallel to one of the principal susceptibilities (k_1, k_2, k_3) (Borradaile and Jackson, 2004). Relations between monoclinic crystals (*a b c,* Fig. 3) and AMS tensor can be described as 'normal' or 'inverse' (Borradaile and Jackson, *in press*). 'Normal' relations include k_{min} // c and k_{max} // a or b (Figs. 3c-d), while 'inverse' relations show k_{min} // b or a and k_{max} // c (Figs. 3e-f). These configurations were used during calculation to better reproduce measured AMS. And example of that procedure is presented in Sample *LF1* (Figs.4c-f)

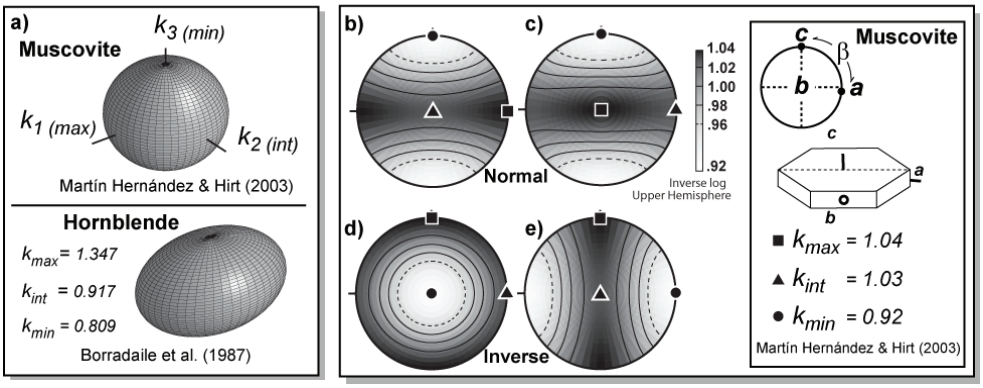

Figure 3. a) AMS ellipsoid for muscovite and hornblende single crystals. b)-e) Projections of single crystal AMS tensor for muscovite; b) and c) are 'normal' relations between monoclinic crystal axes (*abc*) and AMS tensor axes *(k_{max}, k_{int}, k_{min})*, d) and e) describe the 'inverse' relations. After Borradaile and Jackson (*in press*). See the text for a discussion.

It is important to note that for monoclinic crystals the data of physical properties are commonly given in the second setting, so we have first transformed them into the first setting with equation (29) from Matthies and Wenk (2009). After that, aggregate magnetic properties for muscovite and hornblende aggregates were calculated by averaging single crystal AMS over the first setting OD in BEARTEX (Wenk et al. 1998). Results were plotted through VELO routine in BEARTEX. Alternatively OD can be recalculated with MTEX (Hielscher and Schaeben, 2008) from MAUD pole figures. MTEX data can be processed and plotted on T2 software (Mainprice, 1990). Well known averaging schemes include Voigt, Reuss, Voigt-Reuss-Hill (VRH) and Geometric Mean (GM) (e.g. Mainprice and Humbert, 1994). We use the Geometric Mean (Matthies et al., 2001), but and example is presented for all the schemes with similar results (Fig. 4c).

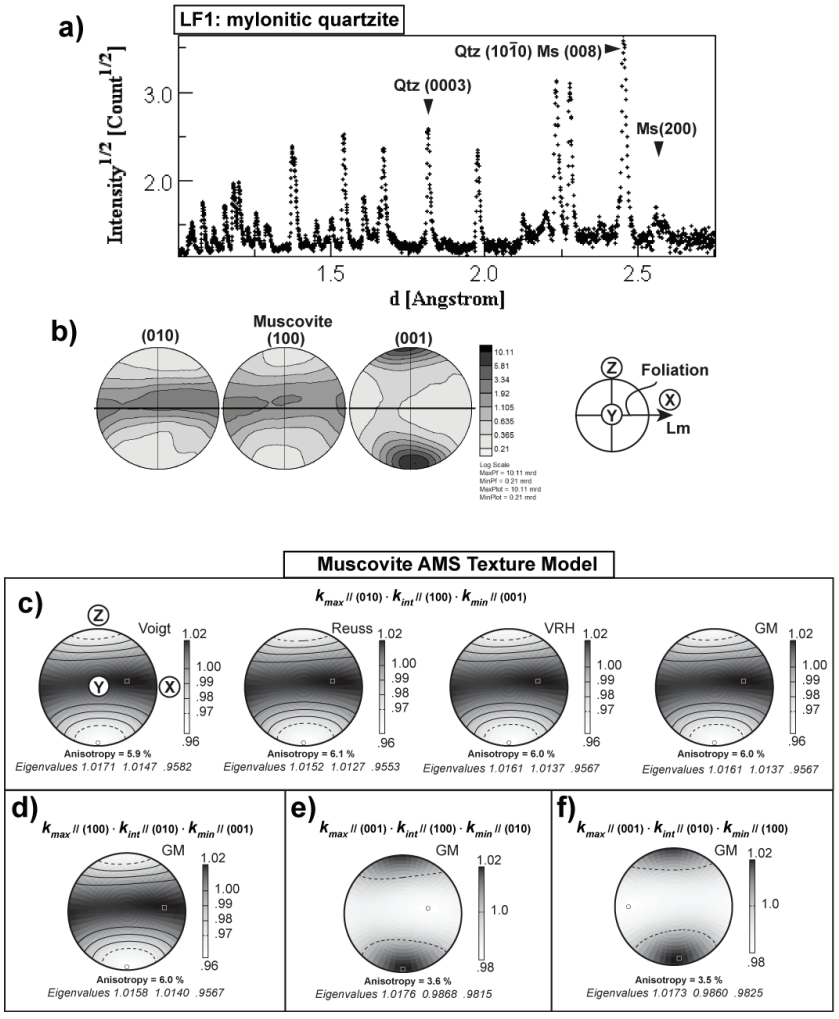

Figure 4. Mylonitic quartzite *LF1*. a) TOF neutron diffraction spectrum from HIPPO 150 bank, some peaks are labeled. b) Muscovite pole figures and reference system. Texture derived AMS for muscovite aggregate. 'Normal' (c-d) and 'inverse' (e-f) configuration (Fig. 3 scheme). In c) four averaging schemes are plotted with similar results. VRH= Voigt-Reuss-Hill, GM= Geometric Mean, Lm= mineral lineation, Qtz= quartz, Ms= Muscovite.

4. RESULTS

4.1. Texture analysis

LF1: Mylonitic quartzite

Muscovite shows a strong texture (~10 m.r.d). It reproduces microstructural observations (Fig. 4b). Basal plane (001) poles define a maximum parallel to the foliation pole (Z), slightly deformed to Y. Deviations from Z axis are probably due to small deflections of grains around quartz grains. (010) and (100) poles appear distributed in asymmetric single girdles, approximately parallel to the foliation plane. (010) and (100) maximum locate at an acute angle to the lineation (X).

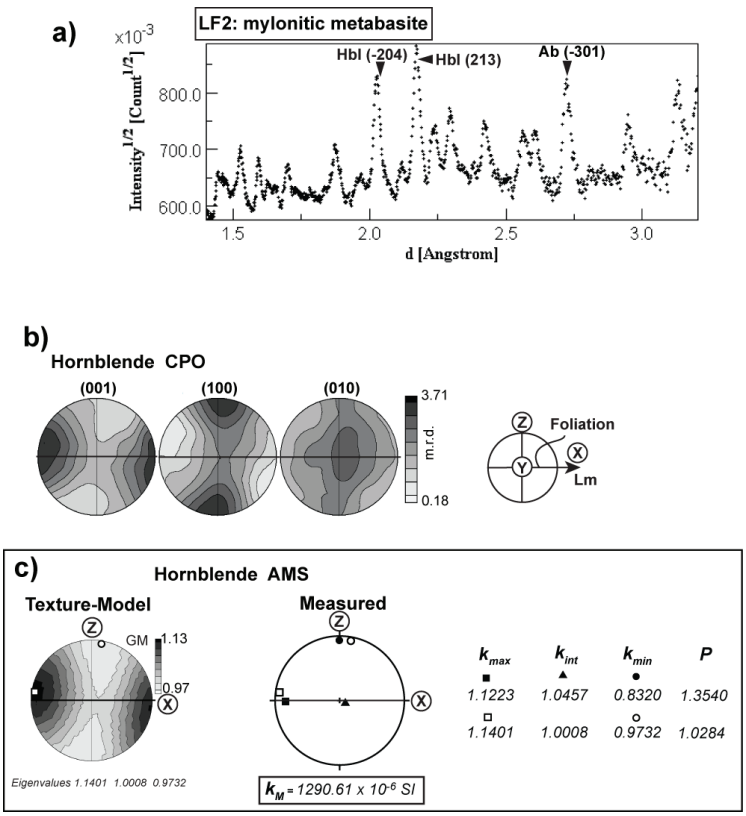

Figure 5. Mylonitic metabasite *LF2*. a) TOF neutron diffraction spectrum from HIPPO 90 bank, some important peaks are indexed. b) Hornblende pole figures and reference system. c) Texture derived AMS for hornblende aggregate and measured AMS of the rock. Principal axes of AMS tensor are indicated. GM= Geometric Mean, Lm= mineral lineation, Hbl= hornblende, Ab= albite. Open symbols = calculated AMS, closed symbols= experimental AMS. k_M = mean susceptibility, P = anisotropy degree (Nagata, 1961)

LF2: Mylonitic metabasite
Hornblende displays an almost orthorhombic moderate texture (3.7m.r.d.) (Fig. 5b). The *c*-axis [001] defines a single maximum almost parallel to the lineation (X) and slightly oblique to the foliation plane (~10º). The distribution of *a*-axis [100] and *b*-axis [010] define incomplete girdles with submaxima parallel to the foliation pole (Z) and Y, respectively

M1: Mylonitic quartzite
Muscovite presents a weak but consistent preferred orientation (1.3 m.r.d.) (Fig. 6b). The basal planes (001) define a wide maximum around foliation pole, but consistently deviated from Z reference axis ~30-35º. Within that angular range, (010) and (100) show a girdle roughly parallel to the foliation plane, but with interesting submaxima located at an acute angle (<45º) to the lineation (X).

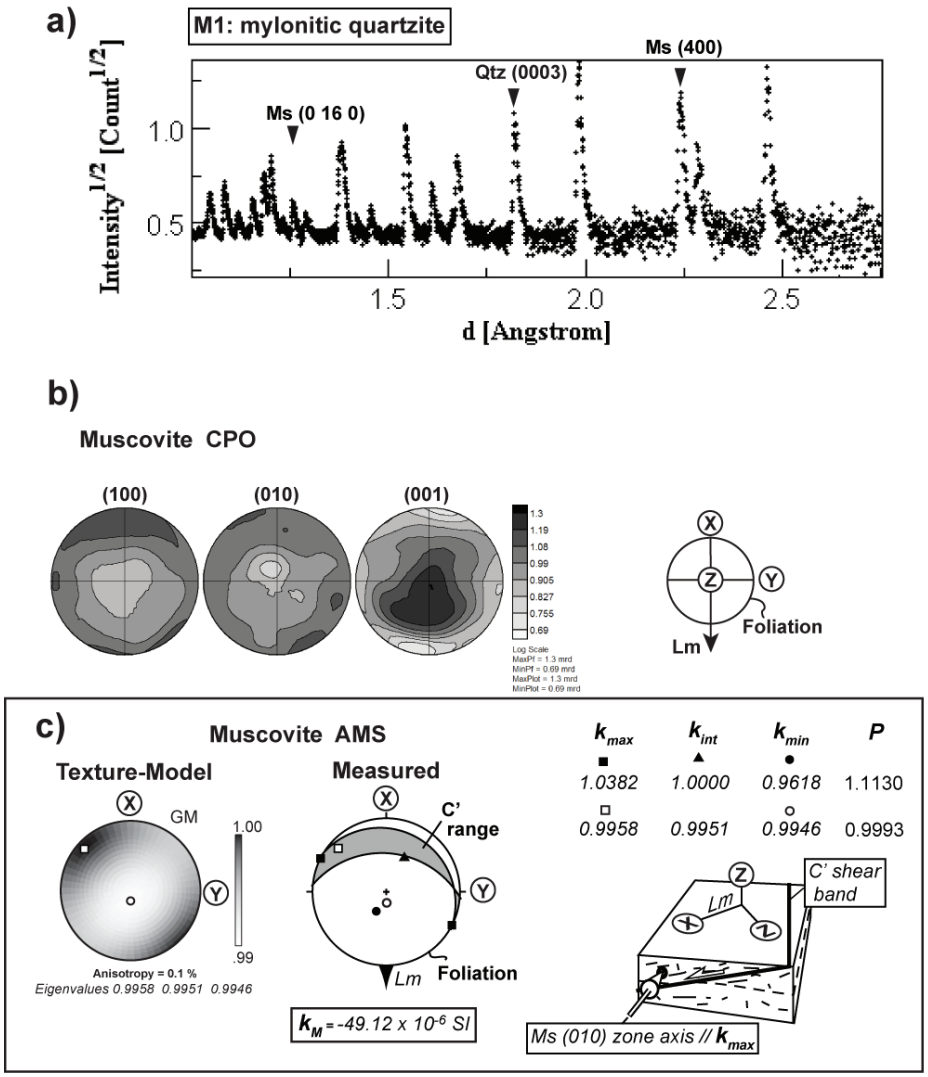

Figure 6. Mylonitic quartzite *M1*. a) TOF neutron diffraction spectrum from HIPPO 150 bank, some important peaks are indexed. b) Muscovite pole figures and reference system (note foliation is now the ecuatorial plane of the projection (XY)). c) Texture derived AMS for muscovite aggregate and measured AMS of the rock. Principal axes of AMS tensor are indicated. Open symbols = calculated AMS, closed symbols= experimental AMS. k_M = mean susceptibility, P = anisotropy degree (Nagata, 1961) Microstructural scheme where shear bands (C') orientation and distribution of muscovite (010) zone axis are represented.

M2: Annealed mylonitic quartzite

In this sample, muscovite presents a very weak texture (1.12 m.r.d.) (Fig. 7b). Statistical distribution (eigenvectors) of maximum and minimum values was plotted in pole figures. Basal planes (001) appear statistically aligned with foliation, while (100) poles define a maximum at ~25º to the lineation (X) and within the foliation plane.

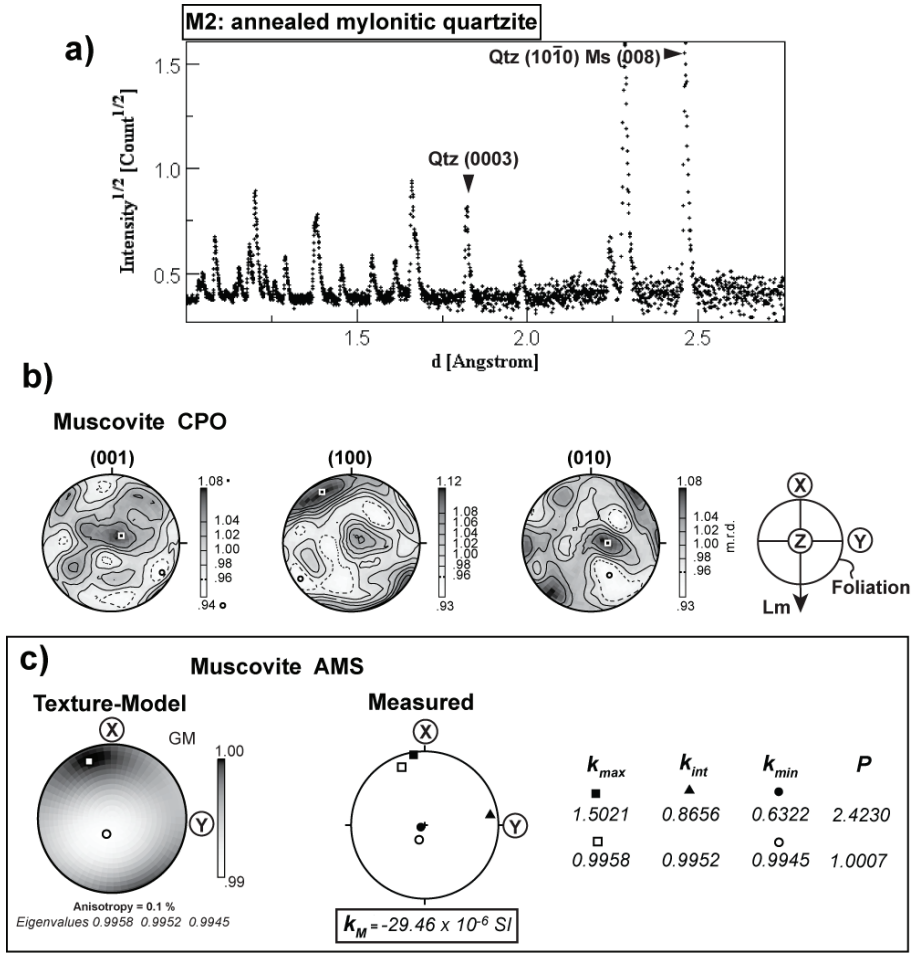

Figure 7. Annealed mylonitic quartzite *M2*. a) TOF neutron diffraction spectrum from HIPPO 150 bank, some important peaks are indexed. b) Muscovite pole figures and reference system (note foliation is now the ecuatorial plane of the projection (XY)). c) Texture derived AMS for muscovite aggregate and measured AMS of the rock. Principal axes of AMS tensor are indicated. Open symbols = calculated AMS, closed symbols= experimental AMS. k_M = mean susceptibility, P = anisotropy degree (Nagata, 1961).

4.2. AMS

AMS is oblate (T = 0.509) for *LF2 sample*, with k_{min} parallel to the foliation pole (Z), and k_{max} at a small angle to the lineation (X). k_{int} is oriented within the foliation plane (Fig. 5c). Mylonitic quartzites from the Lugo Dome show a neutral to slightly prolate AMS (T_{M1} = -0.133; T_{M2} = -0.259). k_{min} in *M1* quartzite is within the foliation plane at 33º to Y reference axis (Fig. 6c), while k_{min} is at 35º to the foliation pole (Z). In sample *M2*, k_{min} is at 7º to the foliation pole (Z), while k_{max} plots at 9º to the rock lineation (X) (Fig. 7c).

Calculated AMS are plotted in Figs. 4c to 7c. Different relations between crystal directions and AMS single crystal tensors were taken into account, and only the best approximations to the measured AMS are presented for each sample. A good correlation exists between calculated and measured AMS axes orientation. However, the degree of anisotropy (P) is not well reproduced in the models.

5. DISCUSSION

Complete orientation distribution (OD) of relevant minerals was obtained after TOF neutron diffraction analysis and Rietveld-based quantitative texture refinement. Volume nature of analytical technique is most appropriate for texture calculations of physical properties of the aggregate (e.g. Ullemeyer et al., 2000). Our results indicate that even low concentration of minerals, with a weak preferred orientation can be de-convoluted with that technique.

In the case of *LF1* quartz mylonite, we have simulated different AMS responses based on quantitative texture analysis. A potential application is the exploration of different synthetic mixtures of micas and other mineral components changing their volume fractions (e.g. Tatham et al. 2008). Mylonitic metabasite (*LF2*) is a complex aggregate of low symmetry phases, so texture analysis itself is a challenge (Gómez Barreiro et al., 2010). Other phases may be contributing to the rock susceptibility with different sign and intensity, however mean susceptibility can be explained by the paramagnetic contribution of amphibole. Unfortunately our knowledge about the relation between single crystal AMS tensor and crystal lattice of silicates is very limited (e.g. Borradaile et al., 1987; Sigamony, 1994; Friederich, 1995; Uyeda et al., 2000; Borradaile and Jackson, 2004), that is why complete AMS simulation of complex polymineralic rocks is not possible yet. Interestingly, texture analysis and AMS simulation demonstrate that inverse relations (Borradaile and Jackson, *in press*) exist between crystal directions and AMS principal axes, where k_{max} // $[001]_{Hornblende}$ hence k_{max} // Lineation (X). This finding is important for correlation of AMS measurements and microstructure. Alternatively ferromagnetic microinclusions in amphibole might be modifying crystal to AMS relations (e.g. Lagroix and Borradaile, 2000; Feinberg et al., 2005).

In rocks with a very low magnetic susceptibility we can assume that even very small fractions of paramagnetic minerals may control bulk AMS (Rochette, 1987; Cifelli et al., 2009). This is the case of Lugo Dome mylonites. Diamagnetic quartz dominates the fabric (Figs. 6-7). However, the orientation of measured and calcu-

lated AMS tensor agree quite well, indicating a 'normal' relation between crystal axes and AMS tensor. It is suggested that muscovite fabrics can be mapped with AMS technique across the shear zone. In the case of active domains in the shear zone (mylonite *M1*), new information has been revealed with AMS analysis. The k_{max} // [100] $_{\text{Muscovite}}$, and is included in the mylonitic foliation, while k_{min} // $[001]_{\text{Muscovite}}$. The angular relationship between fabric elements (foliation and lineation) and AMS correlates with microstructural and field observation of shear-band (C') development (Fig. 6c). AMS analysis has confirmed kinematic criteria in the shear zone. Sample *M2*, represents a domain of the shear zone where intense annealing has removed shape fabric, and structural correlation is difficult. Our results demonstrate that relic fabric preserved within cm quartz grains can by investigated with AMS. It should be noticed that for the same sample volume, orientation of muscovite relic foliation is better defined by AMS than by neutron diffraction (Fig. 7).

6. CONCLUSIONS

The orientation of minerals in an aggregate has a profound influence on physical properties of the rock, most importantly, anisotropy. Quantitative texture analysis with TOF neutron diffraction technique has unique advantages because of high penetration in geomaterials. The Rietveld method, as implemented in the software MAUD has proved to be a very powerful tool to retrieve orientation distribution of minerals from complex materials, like metabasites.

AMS can be calculated by averaging single crystal AMS tensor over the orientation distribution of the aggregate. Orientation of measured and calculated AMS tensors agree quite well, but shape factors and anisotropy degree show great discrepancy. It is suggested that other magnetic sources (diamagnetic, paramagnetic, ferromagnetic) are contributing to the bulk AMS. The relation between AMS principal axes and monoclinic lattices is solved by AMS models. As a result, an apparent 'inverse' relation has been established for hornblende. Low field AMS is a useful tool to combine with texture analysis to shed light on otherwise hidden fabrics.

7. ACKNOWLEDGEMENTS

We thank F. Martín-Hernández for the invitation to participate in this special issue. H.-R. Wenk and S. Vogel are thanked for continuous support and discussions about texture and neutron diffraction. R. Hielscher made insightful comments about MTEX. D. Mainprice is thanked for providing T2 software. This work was supported by the Dirección General de Programas y Transferencia del Conocimiento (Spanish Ministry of Science and Innovation), Research Projects no. CGL2007-65338-CO2-01 and 02/BTE. Access to LANSCE (HIPPO) to perform texture measurements was invaluable. JGB was supported by a Juan de la Cierva postdoctoral contract (MEC).

8. REFERENCES

BABUŠKA, V., & PLOMEROVÁ, J., (2006). European mantle lithosphere assembled from rigid microplates with inherited seismic anisotropy, *Phys. Earth Planet. Inter.* 158: 264–280.

BORRADAILE, G.J., (1988). Magnetic susceptibility, petrofabrics and strain. *Tectonophysics*, 156: 1-20.

BORRADAILE, G.J., KEELER, W., ALFORD, C. & SARVAS, P. (1987). Anisotropy of magnetic susceptibility of some metamorphic minerals. *Phys. Earth Planet. Interior*s. l2: 215-222. .

BORRADAILE, G.J., & JACKSON, M. (2004). Anisotropy of magnetic susceptibility (AMS): magnetic petrofabrics of deformed rocks. *In*: Martín-Hernández, F., Lüneburg, C.M., Aubourg, C., and Jackson, M., (eds.): *Magnetic Fabric: Methods and Applications*. Geological Society, London, Spec. Pub., 238, 299-360.

BORRADAILE, G.J., & JACKSON, M., (*in press*). Structural geology, petrofabrics and magnetic fabrics (AMS, AARM, AIRM), *Journal of Structural Geology*, DOI: 10.1016/j.jsg.2009.09.006.

BORRADAILE, G.J., & WERNER, T., 1994. Magnetic anisotropy of some phyllosilicates. *Tectonophysics* 235, 223–248.

CHRISTENSEN, N.I. (1971), Shear wave propagation in rocks, *Nature,* 229:549-550

CIFELLI, F., MATTEI, M., CHADIMA, M. LENSER, S., & HIRT, A.M. (2009). The magnetic fabric in 'undeformed clays': AMS and neutron texture analyses from the Rif Chain (Morocco), *Tectonophysics*, 466: 79-88.

DÍEZ FERNÁNDEZ, R., MARTÍNEZ CATALÁN, J.R. (2009) 3D Analysis of an Ordovician igneous ensemble: A complex magmatic structure hidden in a polydeformed allochthonous Variscan unit, *Journal of Structural Geology*, 31: 222-236

FEINBERG, J., SCOTT, G.R., RENNE, P., & WENK, H.-R., (2005). Exsolved magnetite inclusions in silicates: Features determining their remanence behavior. *Geology* 33, 513-516.

FEINBERG, J., WENK, H.-R., SCOTT, G.R., & RENNE, P., (2006). Preferred orietation and anisotropy of physical properties in gabbros from the Bushveld complex. *Tectonophysics,* 420, 345-356.

FRIEDERICH, D., 1995, Gefügeuntersuchungen an Amphiboliten der Bhómishen Masse unter besonderer Berücksichtigung der Anisotropie der magnetischen Suszetibiltät. *Geotektonische Forschungen*, 82: 1-118.

GÓMEZ BARREIRO, J., LONARDELLI, I., WENK, H.-R., DRESEN, G., RYBACKI, E., REN, Y., TOME, C.T. (2007) Preferred orientation of anorthite deformed experimentally in Newtonian creep. *Earth and Planetary Science Letters,* 264, 188-207.

GÓMEZ BARREIRO J., MARTÍNEZ CATALÁN, J.R., PRIOR, D., WENK H.-R., VOGEL S., DÍAZ GARCÍA F., ARENAS R., SÁNCHEZ MARTÍNEZ S., LONARDELLI I. (2010). Fabric development in a Middle Devonian intra-oceanic subduction regime: The Careon ophiolite (NW Spain). *J. Geology* 118, 163-186..

HIELSCHER, R. & SCHAEBEN, H. (2008) A novel pole figure inversion method: specification of the MTEX algorithm *J. Appl. Cryst*. (2008). 41, 1024-1037

HOBBS, B.E., MEANS, W.D., WILLIAMS, P.F., (1976) *An outline of Structural Geology*. Wiley, New York, 571 pp.

HROUDA, F., (1986). The effect of quartz on the magnetic anisotropy of quartzite. *Studia Geophysica et Geodaetica* 30, 39-45.

JELINEK, V. (1981), Characterization of the magnetic fabric of rocks. *Tectonophysics*, 79: 63-67.

KARATO, S.-I. (1998) Seismic Anisotropy in the Deep Mantle, Boundary Layers and the Geometry of Mantle Convection *Pure Appl. Geophys.* 151: 565–587

KERN, H., & WENK, H.-R. (1985): Anisotropy in rocks and the geological significance, *In:* Wenk, H.-R. (ed.), *Preferred orientation in deformed metals and rocks: an introduction to modern texture analysis*, Academic Press, 601 pp.

KERN, H.M., (1993), Physical properties of crustal and upper mantle rocks with regards to lithosphere dynamics and high pressure mineralogy, *Physics of the Earth and Planetary Interiors*, 79:113—136.

KOCKS, U.F., TOMÉ C., & WENK, H.-R. (2000). Texture and Anisotropy. Preferred Orientations in Polycrystals and Their Effect on Materials Properties. 2nd paperback edition. Cambridge University Press, 676pp.

LAGROIX, F., & BORRADAILE, G.J., (2000). Magnetic fabric interpretation comnplicated by inclusions in mafic silicates. *Tectonophysics*, 325: 207-225.

LEISS, B., GROGER, H. R., ULLEMEYER, K., & LEBIT, H. (2002). Textures and microstructures of naturally deformed amphibolites from the northern Cascades, NW USA: methodology and regional aspects *Geological Society, London, Special Publications*, 200: 219-238

LONARDELLI, I., WENK, H.-R., LUTTEROTTI, L. & GOODWIN, M. (2005).Texture analysis from synchrotron diffraction images with the Rietveld method: Dinosaur tendon and salmon scale. *J. Synchr. Research* 12, 354-360.

LUTTEROTTI, L., S. MATTHIES & H.-R. WENK (1999), MAUD: a friendly Java program for materials analysis using diffraction, *Int. U. Crystallogr. Comm. Powder Diffraction Newsletter*, *21*, 14 - 15.

MAINPRICE, D. & HUMBERT, M. (1994) Methods of calculating petrophysical properties from lattice preferred orientation data. *Surveys in Geophysics* 15, 575-592

MAINPRICE D. (1990). An efficient fortran program to calculate seismic anisotropy from the lattice preferred orientation of minerals. *Computers & Gesosciences*,16,385-393.

MAINPRICE, D., BARRUOL, G., & BEN ISMAIL, W.,(2000)- The seismic anisotropy of the Earth's mantle: from single crystal to polycrystal. In: S.I. Karato, Editor, *Earth's Deep Interior: Mineral Physics and Tomography from the Atomic to the Global Scale*, *Geodyn. Ser.*, AGU, Washington, D.C. 237–264.

MARTÍNEZ CATALÁN, J.R., ARENAS, R., & DÍEZ BALDA, M.A. (2003), Large extensional structures developed during emplacement of a crystalline thrust sheet: the Mondonedo nappe (NW Spain), *Journal of Structural Geology*, 25: 1815-1839

MARTÍNEZ CATALÁN, J.R., ARENAS, R., ABATI, J., SÁNCHEZ MARTÍNEZ, S., DÍAZ GARCÍA, F., FERNÁNDEZ-SUÁREZ, J., GONZÁLEZ CUADRA, P., CASTIÑEIRAS, P., GÓMEZ BARREIRO, J., DÍEZ MONTES, A., GONZÁLEZ CLAVIJO, E., RUBIO PASCUAL, F.J., ANDONAEGUI, P., JEFFRIES, T.E., ALCOCK, J.E., DÍEZ FERNÁNDEZ, R. AND LÓPEZ CARMONA, A. (2009) A rootless suture and the loss of the roots of a mountain chain: the Variscan belt of NW Iberia. *Comptes Rendus Geoscience de l'Académie des sciences*, 341, 114-126.

MARTÍN-HERNÁNDEZ, F., & HIRT, A.M., (2003). The anisotropy of magnetic susceptibility in biotite, muscovite and chlorite single crystals. *Tectonophysics*, 367, 13–28.

MARTÍN-HERNÁNDEZ, F., LUNEBURG, C.M., AUBOURG, C. AND JACKSON, M. (Eds.) (2004), Magnetic Fabric: Methods and Applications. *Geological Society, London, Special publications,* 238.

MARTÍN-HERNÁNDEZ, F., KUNZE, K., JULIVERT, M., AND HIRT A.M. (2005). Mathematical simulation of magnetic susceptibility on composite fabrics, *J. Geophys. Res., 110, B06102, doi: 10.1029/2004JB003505, 2005*

MATTHIES, S., PRIESMEYER, H.G., & DAYMOND, M.R., (2001): On the diffractive determination of single-crystal elastic constants using polycrystalline samples. *J. Appl. Cryst.* 34: 585-601

MATTHIES, S., PEHL, J., WENK, H.-R., & VOGEL, S., (2005). Quantitative texture analysis with the HIPPO TOF diffractometer. *J.Appl. Cryst*. 38: 462-475.

MATTHIES S. & WENK H.-R (2009). Transformations for monoclinic crystal symmetry in texture analysis. *J. Appl. Cryst.* 42: 564-571.

NAGATA, T., 1961, *Rock Magnetism*, Maruzen, Tokyo, p. 350.

NICOLAS, A. & CHRISTENSEN, N.I. (1987). Formation of anisotropy in upper mantle peridotites—A review. In: K. Fuchs and C. Froideveaux, Editors, *Composition Structure and Dynamics of the Lithosphere Asthenosphere System*, AGU, Washington D.C., 111–123.

OWENS, W.H., (1974). Mathematical model studies on factors affecting the magnetic anisotropy of deformed rocks. *Tectonophysics*, 24: 115–131.

PARK, J., & LEVIN, V. (2002) Geophysics–seismic anisotropy: tracing plate dynamics in the mantle, *Science* 296: 485–489

PRIOR, D.J., A.P. BOYLE, F. BRENKER, M.C. CHEADLE, A. DAY, G. LÓPEZ, L. PE-RUZZO, G.J. POTTS, S. REDDY, R. SPIESS, N.E. TIMMS, P. TRIMBY, J. WHEELER AND L. ZETTERSTRÖM (1999), The application of electron backscatter diffraction and orientation contrast imaging in th SEM to textural problems in rocks, *Am. Mineral.*, 84: 1741 - 1759.

ROCHETTE, P., (1987). Metamorphic control of the magnetic mineralogy of black shales in the Swiss Alps: toward the use of "magnetic isograde", *Earth and Planetary Science Letters*, 84: 446-45~

SAVAGE, M.K., & SILVER, P.G., (1993) Mantle deformation and tectonics: constraints from seismic anisotropy in western United States, *Phys. Earth Planet. Inter.* 78: 207–227.

SIEGESMUND, S., ULLEMEYER, K., DAHMS, M., 1995, Control of magnetic rock fabrics by mica preferred orientation: a quantitative approach, *Journal of Structural Geology*, 17: 1601-1613.

SIGAMONY, A., (1994). The magnetic properties of tourmaline and epidote. *Proceedings Mathematical Sciences*, 20: 200-2003.

SCHMIDT, V., HIRT, A.M., LEISS, B., BURLINI, L., & WALTER, J.M., 2009, Quantitative correlation of texture and magnetic anisotropy of compacted calcite–muscovite aggregates, *Journal of Structural Geology*, 31: 1062–1073

TARLING, D. H., & HROUDA, F., (1993). *The Magnetic Anisotropy of Rocks*. Chapman, Hall, London, 217 pp.

TATHAM, D.J., LLOYD, G.E., BUTLER, R.W.H., CASEY, M. (2008), Amphibole and lower crustal seismic properties, *Earth and Planetary Science Letters*, 267, 118 – 128.

ULLEMEYER, K., BRAUN, G., DAHMS, M., KRUHL, J.H., OLESEN, N., SIEGES-MUND, S. (2000), Texture analysis of a muscovite-bearing quartzite: a comparison of some currently used techniques, *Journal of Structural Geology*, 22: 1541 – 1557.

UYEDA, CH., OHTAWA, K., OKITA, K, (2000), Diamagnetic anisotropy of silicates composed of tetrahedral networks. *J.Phys. Soc. Jpn.*, 69: 1019-1022.

VOGEL, S.C., PRIESMEYER, H.-G. (2006), Neutron production , neutron facilities and neutron instrumentation., in Wenk, H.-R., (ed.): *Neutron scattering in Earth sciences*, Rev. Min. Geochem. MSA, 63: 27-57.

WENK, H.-R. (1985). Edit. Preferred Orientation in Deformed Metals and Rocks. An Introduction to Modern Texture Analysis, Academic Press.

WENK, H.-R., MATTHIES, S., DONOVAN, J. & CHATEIGNER, D. (1998). BEARTEX, a Windows-based program system for quantitative texture analysis. J. Appl. Cryst. 31, 262-269.

WENK & S. GRIGULL (2003). Synchrotron texture analysis with area detectors. *J. Appl. Cryst.* 36, 1040-1049.

WENK, H.-R., LUTTEROTTI, L., GRIGULL,S., VOGEL, S., (2003). Texture analysis with the new HIPPO TOF diffractometer. *Nucl. Instr. Methods* A515, 575-588.

WENK, H.R. AND CHRISTIE, J.M. (1991). Comments on the interpretation of deformation textures in rocks. *Journal of Structural Geology*, 13: 1091-1110.

WENK, H.-R., & VAN HOUTTE, P., (2004). Texture and Anisotropy. *Reports on Progress in Physics* 67, 1367-1428.

WENK, H.-R., VOLTOLINI, M., KERN, H., POPP, H. & MAZUREK, M. (2008). Anisotropy of Mont Terri Opalinus Clay. *The Leading Edge* 27, 742-748.

WENK, H-R, VOLTOLINI, M., MAZUREK, M., VAN LOON, L.R., & VINSOT, A. (2008). Preferred orientations and anisotropy in shales: Callovo-Oxfordian shale (France) and Opalinus Clay (Switzerland). *Clays and Clay Minerals* 56, 285-306.

XIE, Y., WENK, H.-R., & MATTHIES, S., (2003). Plagioclase preferred orientation by TOF neutron diffraction and SEM-EBSD. *Tectonophysics* 370, 269-286.